Enhanced Heat Transfer, 2001, Vol. 8, pp. 243–259
Reprints available directly from the publisher
Photocopying permitted by license only

Modeling the *f* and *j* Characteristics for Transverse Flow Through an Offset Strip Fin at Low Reynolds Number

Y. S. MUZYCHKA[a,*] and M. M. YOVANOVICH[b]

[a]*Faculty of Engineering and Applied Science, Memorial University of Newfoundland, St. John's, Newfoundland, Canada, A1B 3X5;* [b]*Department of Mechanical Engineering, University of Waterloo, Waterloo, Ontario, Canada, N2L 3G1*

(Received 2 January 2001; In final form 9 January 2001)

Analytic models for predicting the thermal-hydraulic characteristics for transverse flow through an offset strip fin array are developed. These models are developed by combining the creeping or low flow asymptotic behaviour with laminar and turbulent boundary layer wake models. Expressions for each of these characteristic regions are developed using fundamental solutions of fluid dynamics and heat transfer. The proposed models are compared with new experimental data for ten offset strip fin configurations. Model predictions are within ± 20 percent for 92 percent of friction factor data and 71 percent for Colburn *j* factor data.

Keywords: Compact heat exchangers; Heat transfer coefficient; Friction factor; Extended surface; Modelling

INTRODUCTION

Many automotive oil coolers use compact extended surfaces often referred to as "turbulator" strips, as a means of heat transfer enhancement. A turbulator strip is essentially an offset strip fin oriented normal to the flow rather than parallel to the flow. These devices provide enhancement by means of increased surface area along with larger heat transfer coefficients due to the complex flow field. In many applications the designer must optimize heat transfer for a given pumping power, mass flow rate or pressure drop. Optimization of a new design incorporating these devices is best achieved with analytic or empirical models. Unfortunately, due the proprietary nature of these devices, details of thermal and hydraulic performance are not published, Webb (1994). As a result of the lack of published data, no models or data are readily available in the open literature.

In applications involving turbulator strips, the only available design data are the numerical

*Corresponding author. e-mail: yuri@engr.mun.ca

studies of Patankar *et al.* (1977) and Sridhar (1995). Patankar *et al.* (1977) used numerical methods to predict heat transfer and pressure drop for transverse flow through an array of interrupted plates. However, this configuration assumed a large channel height such that three dimensional effects were not present. These results are valid over a moderate range of Reynolds numbers, however, they are only valid for flows which are two dimensional. In most practical applications, the flow is three dimensional and the effect of the channel walls is to reduce the overall enhancement.

This paper develops an analytic model and presents experimental data for a number of turbulator strip configurations. This new data is used in conjunction with the analytical model development. Simple analytic models have been developed for the laminar wake and turbulent wake regions which accurately predict the Fanning friction factor, f, and the Colburn j factor for the turbulator strip. The asymptotic models are then combined using the Churchill and Usagi (1972) correlation method to provide a model which is valid over the entire range of Reynolds number. A comparison of the new model with experimental data shows agreement within $+/-20$ percent for 92 percent of the f data and 71 percent of the j data.

REVIEW OF PUBLISHED MODELS

In many of the reviews on enhanced heat transfer (Bergles, 1985; Webb, 1987; Webb, 1994; Kalinin and Dreitser, 1998) an abundance of data is available for many common enhancements such as rib turbulators, internally finned tubes and channels, louvered fins, and offset strip fins. Many automotive heat exchangers employ turbulator strips and other enhanced heat transfer technology as a means of enhancing heat transfer. However, as discussed by Webb (1994) most of the enhanced heat transfer surfaces employed by the automotive industry are considered proprietary technology, and details of the heat transfer and fluid friction characteristics are not published.

Patankar *et al.* (1977) used numerical methods to solve the two dimensional transverse flow through an array of staggered plates. However, this configuration assumed a large channel height such that three dimensional effects were not present. The data of Patankar *et al.* (1977) for a configuration having fins of width and spacing equal to L_f in both parallel and transverse directions have been digitized and correlated by the following expressions:

$$f = 2.31\left(Re_{L_f}\right)^{0.1} \tag{1}$$

for the friction factor, and

$$j_R = 0.294\left(Re_{L_f}\right)^{-0.3013} \tag{2}$$

and

$$j_F = 2.814\left(Re_{L_f}\right)^{-0.5642} \tag{3}$$

and

$$j_A = 1.246\left(Re_{L_f}\right)^{-0.4753} \tag{4}$$

for the Colburn j factor, where the subscripts F, R, and A represent the front, rear and average values for the obstruction, respectively, and $Re_{L_f} = \overline{w}L_f/\nu$. The Reynolds number range is limited to $200 < Re < 2000$. Since these results are based upon a two dimensional system, the effect of the channel height H, would be to reduce the overall enhancement. Thus, based upon the work of Patankar *et al.* (1977), Eq. (4) is the theoretical maximum value for the Colburn j factor for transverse flow through the array. Comparison of Eq. (4) with the solution for parallel flow past a flat plate shows that a twofold increase in the heat transfer coefficient is possible for transverse flow. Finally, the friction factor is approximately independent of the Reynolds number, indicating that almost all of the pressure drop is due to form drag.

MODEL DEVELOPMENT

In this section the details of the model development for the turbulator strip geometries are discussed. A typical turbulator strip geometry is shown in Figure 1. The turbulator may be characterized by the fin width W or alternatively fin length L_f for parallel flow, the channel height H, the wavelength λ, the fin thickness t, and fin angle θ. If the turbulator strip profile is sinusoidal rather than square or trapezoidal, then the fin angle is not constant. However, it may be nominally defined as:

$$\theta = \tan^{-1}(2H/\lambda) \tag{5}$$

The models developed in this section will be compared with experimental data for ten turbulator geometries provided in Muzychka (1999). The following assumptions are made in the model development: ideal surfaces *i.e.*, no burrs or scarfed edges, uniform surface dimensions throughout the array, large separation/recirculation zone in the rear of each fin, negligible edge contributions, perfect contact at channel walls, and isothermal surfaces. In general, the presence of burrs will have some effect on the thermal-hydraulic characteristics, however, the devices considered later in this work were free of significant burring.

Models will be developed for creeping or low flow, laminar boundary layer flow, and turbulent boundary layer flow regions. The laminar and turbulent flow asymptotes will then be combined with the creeping flow asymptote using the Churchill and Usagi (1972) asymptotic correlation method in the form:

$$f = \left[\{(f_{cf})^m + (f_{\text{lam}})^m\}^{n/m} + (f_{\text{tur}})^n\right]^{1/n} \tag{6}$$

and

$$j = \left[(j_{cf})^p + \{(j_{\text{lam}})^q + (j_{\text{tur}})^q\}^{p/q}\right]^{1/p} \tag{7}$$

where m, n, p, and q are correlation parameters to be chosen based upon comparisons with the experimental data. Eqs. (6) and (7) provide models which are valid for all Reynolds numbers.

The laminar and turbulent flow region models will be developed by considering force and energy balances on a simple control volume. A friction factor model for the turbulator geometry shown in Figure 1 may be developed by performing a simple force balance on a basic element or repeating cell which is shown below in Figure 2.

Using a basic cell of dimensions $2W \times \lambda/2 \times H$, a force balance gives:

$$\frac{\overline{\tau}}{(1/2)\rho\overline{w}^2} = \frac{\tau_{\text{walls}}}{(1/2)\rho\overline{w}^2}\left(\frac{A_{\text{walls}}}{A_{\text{wet}}}\right) + \frac{\tau_{\text{fins}}}{(1/2)\rho\overline{w}^2}\left(\frac{A_{\text{fins}}}{A_{\text{wet}}}\right) + C_D\left(\frac{A_{\text{drag}}}{A_{\text{wet}}}\right) + K_{\text{eff}}\left(2\frac{A_{\text{front}}}{A_{\text{wet}}}\right) \tag{8}$$

where $A_{\text{walls}} = 2W\lambda$, $A_{\text{fin}} = A_{\text{wet}} - A_{\text{walls}}$, $A_{\text{front}} = 2WH$, $A_{\text{drag}} = WH$ is the characteristic area that the drag coefficient is based upon, and

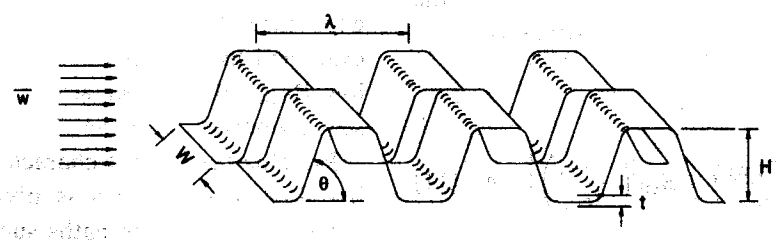

FIGURE 1 Turbulator geometry.

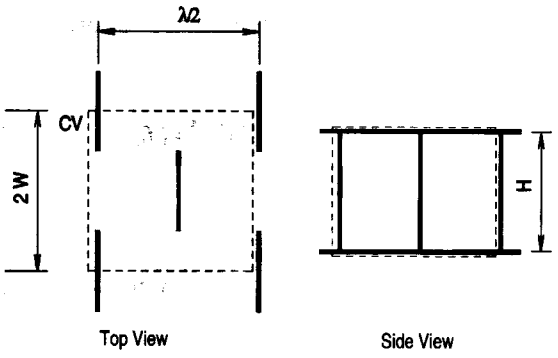

FIGURE 2 Basic cell of turbulator strip.

$A_{wet}=(2\lambda W)F_w$ is the total wetted surface area, and F_w is the area scale factor. The above expression may be written in terms of the friction coefficients for the fin surface and the channel walls:

$$f=f_{walls}\left(\frac{A_{walls}}{A_{wet}}\right)+f_{fins}\left(\frac{A_{fins}}{A_{wet}}\right)+C_D\left(\frac{A_{drag}}{A_{wet}}\right)+K_{eff}\left(2\frac{A_{front}}{A_{wet}}\right) \quad (9)$$

Since the drag and expansion/contraction coefficients are related to the fin surface they may be combined with the fin skin friction term in the following manner:

$$f=f_{walls}\left(\frac{A_{walls}}{A_{wet}}\right)+\left[f_{fins}+C_D\left(\frac{A_{drag}}{A_{fins}}\right)+K_{eff}\left(2\frac{A_{front}}{A_{fins}}\right)\right]\left(\frac{A_{fins}}{A_{wet}}\right) \quad (10)$$

The above expression represents an overall force balance on an element of the turbulator geometry. Now using the characteristic dimensions of the control volume, Eq. (10) may be written as:

$$f=f_{walls}\left(\frac{1}{F_w}\right)+\left[f_{fins}+C_D\left(\frac{A_{drag}}{A_{fins}}\right)+K_{eff}\left(\frac{A_{front}}{A_{fins}}\right)\right]F_f \quad (11)$$

where $F_w=A_{wet}/A_{walls}$ and $F_f=A_{fins}/A_{wet}$.

Equation (11) is valid for both laminar and turbulent flow behavior. However, in the laminar region the C_D and K_{eff} terms are ignored as they only become significant at larger flow rates.

A similar procedure is used to obtain a model for the Colburn j factor as used for the Fanning friction factor. Performing an energy balance on the same basic cell results in the following expression for the average heat transfer coefficient:

$$\bar{h}A_{wet}=\bar{h}_{walls}A_{walls}+\bar{h}_{fins}A_{fins} \quad (12)$$

Equation (12) may be written in terms of the Colburn j factor and the area enhancement factor F_w:

$$j=j_{wall}((1/F_w))+j_{fins}F_f \quad (13)$$

Equation (13) is valid for both laminar and turbulent flow behavior. Expressions will be developed for the Fanning friction factor and the Colburn j factor on the channel walls and fin surfaces using fundamental solutions from the heat transfer and fluid dynamics literature.

Creeping Flow Region

Creeping flow characteristics appear in the low Reynolds number region of the turbulator geometries. These geometries are similar to consolidated media consisting of randomly shaped particles or packed columns typically found in the chemical process industries. The turbulator strip forms a continuous matrix surface which results in a complex flow field, refer to Figure 3. All of the experimental data for the various turbulators examined in Muzychka (1999) appear to have a low Reynolds number asymptote which is inversely proportional to the Reynolds number, $f, j \propto 1/Re$. This behavior is characteristic of the creeping flow regime which is observed in channels having complex flow paths such as flow through porous media.

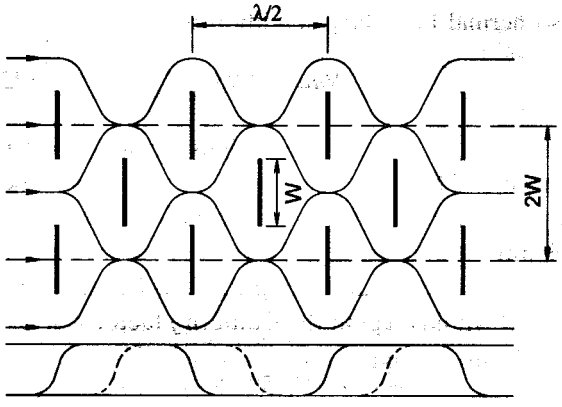

FIGURE 3 Effective flow path.

The friction factor in porous media for $Re \rightarrow 0$ has been derived by Carman (1956) using the Darcy flow model for a circular duct. The expression for the friction factor is usually presented in terms of an equivalent particle diameter. Since the turbulator strip is a continuous matrix, it is more appropriate to use a form which includes the hydraulic diameter of the channel rather than the equivalent spherical particle diameter. The analysis begins with

$$\frac{\Delta p}{L_e} = k_o \frac{16 \mu w_t}{d_h^2} \tag{14}$$

where k_o is called the Kozeny constant (Happel and Brenner, 1965 and Churchill, 1988) for the packed or porous channel, L_e is the tortuous length of the channel and w_t is the tortuous fluid velocity. The Kozeny constant has a value $k_o = 2$ for circular capillaries and $k_o = 3$ for a slit. For other shapes it typically takes a value somewhere between 1.5 and 3. A value of $k_o \approx 2.5$ is found experimentally for various non-circular capillaries, Carman (1956). Coincidentally, it is the average value of the slit and circular capillaries. Carman (1956) proceeded to introduce the tortuosity, L_e/L, and the tortuous velocity, $w_t = \overline{w}(L_e/L)$, to arrive at

$$\frac{\Delta p}{L_e} = k_o \frac{16 \mu \overline{w}}{d_h^2} \left(\frac{L_e}{L}\right) \tag{15}$$

Now rewriting Eq. (15) in terms of the actual length of the channel or column gives:

$$\frac{\Delta p}{L} = k_o \frac{16 \mu \overline{w}}{d_h^2} \left(\frac{L_e}{L}\right)^2 \tag{16}$$

The product of k_o and $(L_e/L)^2$ has been found experimentally to vary between 4 and 6 (Carman, 1956) and theoretical values for cylinders and spheres are reported by Happel and Brenner (1965) to lie between 4 and 7 for porosities between 0.1 and 0.9. Carman (1956) chose a value of $k_o(L_e/L)^2 \approx 5$ based upon the experimental data for flow of gases through a wide range of spherical, cubical, cylindrical and other non-spherical particles. This leads to

$$f = \frac{40}{Re_{dh}} \tag{17}$$

after introducing the definitions of the Fanning friction factor, the Reynolds number and the effective value of $k_o(L_e/L)^2$. The primary difference between the analysis reported above and that found in the literature (Carman, 1956; Bird *et al.*, 1962; Churchill, 1988) is the introduction of the specific surface and porosity concepts to define an effective particle diameter in place of the hydraulic diameter. This usually results in a slightly more complex expression. The result given by Eq. (17) is generally valid below $Re_{d_h} < 10$. Above this critical value inertial effects become important.

An estimate for turbulator strips for the group $k_o(L_e/L)^2$ may be made by computing the value for the effective or tortuous flow length. In the turbulator strip geometries the fluid must flow around periodic obstacles of width W and spaced $\lambda/2$. A typical flow path shown in Figure 3 may be assumed to follow the wave form

$$f(x) = \frac{W}{2} \sin\left(\frac{4\pi x}{\lambda}\right) \tag{18}$$

Now the effective flow length is the length of arc followed by Eq. (18). Using Eq. (18), the

following expression may be derived for the turbulator strip:

$$k_o\left(\frac{L_e}{L}\right)^2 \approx 2.5\left(\frac{\int_0^\lambda \sqrt{1+f'(x)^2}dx}{\lambda}\right)^2 = C_o \quad (19)$$

Applying Eq. (19) along with the assumption that $k_o \approx 2.5$ results in values of $3.57 < k_o(L_e/L)^2 < 6.42$ for the turbulator geometries summarized in Table I. An average value for all ten turbulators gives $k_o(L_e/L)^2 \approx 4.61$, which is in the range of values typical for many packed beds. The creeping flow model for the turbulator geometry is taken to be:

$$f_{cf} = \frac{8C_o}{Re_{d_h}} \quad (20)$$

where,

$$C_o = \frac{10}{\pi^2}(1+b^2)\mathbf{E}^2\left(\sqrt{\frac{b^2}{1+b^2}}\right) \quad (21)$$

and $\mathbf{E}(\cdot)$ is the complete elliptic integral of the second kind and $b = (2\pi W)/\lambda$.

Heat transfer at low Reynolds numbers in a porous parallel plate channel may be modelled as slug flow in a parallel channel containing no porous insert (Nield and Bejan, 1992). The solution for thermally fully developed flow with isothermal boundary condition is

$$Nu_H = 4.93 \quad (22)$$

where H is the channel height or wall to wall spacing. The slug flow model is applicable since the macroscopic velocity distribution in a porous channel is approximately uniform at every point in the cross-section and along the flow length. In the low Reynolds region the Colburn j factor will take the form:

$$j_{cf} = \frac{4.93}{Re_{d_h}Pr^{1/3}}\left(\frac{d_h}{H}\right) \quad (23)$$

TABLE I Summary of surface characteristics

Device	F_w	F_f	ϕ	S_o	d_h
CPI – 1	1.916	0.4783	0.8769	2.225	2.231
CPI – 2	1.921	0.4190	0.8769	2.225	2.484
CPI – 3	2.383	0.5804	0.8953	1.815	1.822
CPI – 4	2.080	0.5194	0.8869	1.731	2.068
CPI – 5	2.417	0.5863	0.8869	1.850	1.780
SQ – 1	2.049	0.6319	0.9167	3.223	2.729
SQ – 2	1.984	0.6223	0.9089	3.111	2.556
SQ – 3	1.899	0.6096	0.8963	2.968	2.312
SQ – 4	2.457	0.5931	0.9091	2.361	2.067
SQ – 5	2.441	0.5904	0.9091	2.361	2.081

Laminar Region

At larger Reynolds numbers, boundary layers are thinner and the results indicate that the friction factor and Colburn j factor become inversely proportional to the square root of the Reynolds number, $f, j \propto 1/\sqrt{Re}$. Solutions to the laminar boundary layer equations with pressure gradient are reported in all convective heat transfer references (Burmeister, 1993; Bejan, 1995). These solutions may be used as an indication of the effects of fin angle, width, and flow orientation. General expressions for the skin friction and heat transfer for any fin angle with $0 < \beta < 1$ are given below. This range covers the orientation from a flat plate to plane stagnation or a fin angle from 0° to 90°.

The friction coefficient is defined as

$$C_{f,x} = 2f''(0)Re_x^{-1/2} \quad (24)$$

where $f''(0)$ is the solution to the boundary layer equations for the velocity gradient at the wall. It may be accurately approximated by the following equation (Burmeister, 1993)

$$f''(0) = \frac{(1.225\beta + 0.244)^{0.534}}{\sqrt{2-\beta}} \quad (25)$$

for the range $0 < \beta < 1$.

The solution for the local Nusselt number in a wedge flow may be presented in terms of Eq. (25) by the following expression given in Cebeci and Bradshaw (1984) for the range $0<\beta<1$ and $Pr\gg1$

$$Nu_x = 1.12\left\{\frac{2}{2-\beta}\frac{f''(0)}{12}\right\}^{1/3} Pr^{1/3}Re_x^{1/2} \quad (26)$$

This expression reduces to

$$Nu_x = \begin{cases} 0.339Re_x^{1/2}Pr^{1/3} & \text{Flat Plate} \\ 0.661Re_x^{1/2}Pr^{1/3} & \text{Plane Stagnation} \end{cases} \quad (27)$$

Average values of the friction and heat transfer coefficients for one wedge surface are related to the local values by means of the following expressions (Bejan, 1995; Burmeister, 1993)

$$\overline{C}_f = \frac{2}{3m+1}C_{f,x} \quad (28)$$

$$\overline{Nu}_L = \frac{2}{m+1}Nu_x \quad (29)$$

where $m=\beta/(2-\beta)$.

In the turbulator strip geometries, fluid approaches an inclined or vertical surface, but since the flow is constrained by the bounding channel walls, the fluid must flow around the obstruction. This flow field is neither similar nor dissimilar to the Falkner-Skan wedge flows, but possesses characteristics of both the flat plate and plane stagnation configurations, refer to Figure 4.

A composite value for an inclined surface which is bounded by two parallel walls is proposed to take the form:

$$Nu_{\text{eff}} = Nu_{FP}\cos^2(\theta) + Nu_{PS}\sin^2(\theta) \quad (30)$$

and

$$C_{f,\text{eff}} = C_{f,FP}\cos^2(\theta) + C_{f,PS}\sin^2(\theta) \quad (31)$$

where FP denotes the flat plate component and PS denotes the plane stagnation component. These approximate expressions reduce to the flat plate and plane stagnation results as $0<\theta<90°$, and reduce to the arithmetic average at $\theta=45°$.

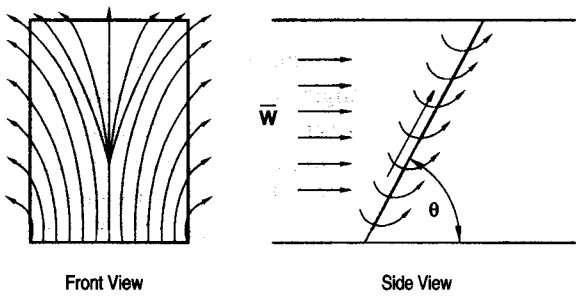

FIGURE 4 Three dimensional flow.

Fluid friction on the channel walls may be modelled as flow over a flat plate. The appropriate expression for predicting the contribution from the channel walls is

$$f_{\text{wall}} = 1.328\left(Re_{d_h}\frac{\lambda}{d_h}\right)^{-1/2} \quad (32)$$

Fluid friction on the inclined fin surface is modelled as a combination of flow over a flat plate and plane stagnation flow. The solution for plane stagnation flow must be presented in terms of the average free stream velocity. Igarashi (1985) determined the appropriate velocity field from experimental measurements on the face of rectangular cylinders and plates oriented normal to a uniform flow field. The local velocity field in the vicinity of the stagnation point varied according to

$$w_\infty(x) = 1.65\frac{\overline{w}x}{W} \quad (33)$$

where W is the width of the plate or rectangular cylinder.

The appropriate expression for predicting the combined effects of plane stagnation and flat plate flow is modelled as

$$f_{fin} = 1.328\left(Re_{d_h}\frac{2S_o}{d_h}\right)^{-1/2}\cos^2(\theta) + 1.538\left(Re_{d_h}\frac{W}{d_h}\right)^{-1/2}\sin^2(\theta) \quad (34)$$

where S_o is the effective fin length.

As the angle of inclination increases to $\theta = 90°$ the expression above reduces to plane stagnation flow, and as the angle decreases the expression tends towards flow over a flat plate. Equation (34) models the leading side of the inclined surface. In the region to the rear, the flow is treated as a separated flow similar to flow past a bluff surface, and it is assumed that the wall shear is equal to zero.

Substituting the laminar boundary layer contributions into Eq. (11) with $K_{\text{eff}} = 0$ and $C_D = 0$ gives:

$$j_{\text{lam}} = \left\{1.328\left(Re_{d_h}\frac{\lambda}{d_h}\right)^{-1/2}\right\}\left(\frac{1}{F_w}\right) + \frac{1}{2}\left\{1.328\left(Re_{d_h}\frac{2S_o}{d_h}\right)^{-1/2}\cos^2(\theta) + 1.538\left(Re_{d_h}\frac{W}{d_h}\right)^{-1/2}\sin^2(\theta)\right\}F_f \tag{35}$$

Heat transfer on the channel walls may be modelled as flow over a flat plate. The appropriate expression for predicting the contribution from the channel walls is

$$j_{\text{wall}} = 0.664\left(Re_{d_h}\frac{\lambda}{d_h}\right)^{-1/2} \tag{36}$$

Heat transfer on the inclined fin surface is modelled as a combination of flow over a flat plate and plane stagnation flow. Once again the plane stagnation flow solution must be converted to a form containing the average free stream velocity. Using Eq. (33), the appropriate expression for predicting the contribution of the fin surface is

$$j = \left\{0.664\left(Re_{d_h}\frac{2S_o}{d_h}\right)^{-1/2}\cos^2(\theta) + 0.849\left(Re_{d_h}\frac{W}{d_h}\right)^{-1/2}\sin^2(\theta)\right\} \tag{37}$$

where S_o is the effective fin length.

As the angle of inclination increases to $\theta = 90°$ the expression above reduces to plane stagnation flow, and as the angle decreases the expression tends towards flow over a flat plate. The above expression models only the leading surface of the fin. In the region to the rear, the flow is treated as a separated flow similar to that in the wake of a bluff body. This flow regime has been modelled analytically as a special case of the Falkner-Skan wedge flows (White, 1991) and has also been examined experimentally (Igarashi *et al.*, 1975). An experimental relation which is valid in the rear of inclined flat plates for $\theta > 10°$, rectangular cylinders and semi-circular cylinders was obtained by Igarashi *et al.* (1975) and is given by

$$Nu_X = 0.191 Re_H^{2/3} Pr^{1/3} \tag{38}$$

where H is the profile height and X is the chord length of the surface in cross-flow. In the present application, the flow in the wake region of the turbulator strip is such, that the chord length and profile height correspond to the width of the obstruction.

The combined effect of the leading and rear faces is simply the arithmetic mean given by

$$j_{\text{fins}} = \frac{1}{2}\left\{0.664\left(Re_{d_h}\frac{2S_o}{d_h}\right)^{-1/2}\cos^2(\theta) + 0.849\left(Re_{d_h}\frac{W}{d_h}\right)^{-1/2}\sin^2(\theta) + 0.191\left(Re_{d_h}\frac{W}{d_h}\right)^{-1/3}\right\} \tag{39}$$

The complete laminar boundary layer model is now given by the following expression:

$$j_{\text{lam}} = 0.664\left(Re_{d_h}\frac{\lambda}{d_h}\right)^{-1/2}\left(\frac{1}{F_w}\right) + \frac{1}{2}\left\{0.664\left(Re_{d_h}\frac{2S_o}{d_h}\right)^{-1/2}\cos^2(\theta) + 0.849\left(Re_{d_h}\frac{W}{d_h}\right)^{-1/2}\sin^2(\theta) + 0.191\left(Re_{d_h}\frac{W}{d_h}\right)^{-1/3}\right\}F_f \tag{40}$$

Turbulent Region

At higher Reynolds numbers the flow becomes highly mixed and although laminar boundary layers may still be formed on the fin surfaces, the flow behaves in a turbulent like manner. Two important solutions which may be used to model the flow characteristics are the friction coefficient for a turbulent boundary layer on a smooth flat surface

$$\overline{C}_f = 0.074 Re_L^{-1/5} \tag{41}$$

and the Nusselt number

$$j = 0.037 Re_L^{-1/5} \tag{42}$$

The above expressions are derived using the 1/7 power law rule for the turbulent velocity distribution. Details of the derivation of these semi-empirical solutions are available in most advanced fluid mechanics and heat transfer texts *e.g.* Schlichting (1979) and Knudsen and Katz (1958).

At higher Reynolds numbers the flow behaves like a turbulent flow with inertial forces being dominant. The contribution of the channel walls to the friction factor may be computed from the following expression presented earlier:

$$f = 0.074 \left(Re_{d_h} \frac{\lambda}{d_h} \right)^{-1/5} \tag{43}$$

On the fin surface, only the form drag and loss coefficients are important. Previous studies by Kays and Crawford (1993) and Joshi and Webb (1987) have suggested that the form drag component in an offset strip fin array may be modelled using the potential flow solution for flow normal to a flat plate. The solution which is reported by both Lamb (1932) and Milne-Thompson (1968) is

$$C_D = \frac{2\pi}{\pi + 4} \approx 0.88 \tag{44}$$

If the fluid flows past an inclined plate the drag coefficient based upon the chord length of the plate as reported by Lamb (1932) and Milne-Thompson (1968) is

$$C_D = \frac{2\pi \sin^2(\theta)}{\pi + 4 \sin(\theta)} \tag{45}$$

Experimental values of the drag coefficient for two dimensional flow normal to flat plates and rectangular cylinders are typically in the range $0.89 < C_D < 2.4$ (Knudsen and Katz, 1958; Blevins, 1984). Experimental results for flow past an inclined plate are also reported in Knudsen and Katz (1958) and Blevins (1984) and vary from $0.2 < C_D < 1.2$ for $20° < \theta < 90°$. Flow past a fin surface within the turbulator geometries is primarily two dimensional since the flow is bound by the channel walls. The effect of fin angle has a considerable effect on the drag coefficient, since part of the flow is over the obstruction and part of the flow is around the obstruction. The following expression is proposed for modelling the drag coefficient

$$C_D \approx 2.4 f(\theta) \tag{46}$$

where

$$f(\theta) = \frac{(\pi + 4) \sin^2(\theta)}{\pi + 4 \sin(\theta)} \tag{47}$$

Equation (47) was obtained by considering the effect of the inclination on the potential flow solution, *i.e.*, Eq. (45) divided by Eq. (44) multiplied by the experimental value for the drag coefficient of a thin rectangular plate oriented normal to the flow $C_D(90°) \approx 2.4$.

Finally, as the fluid flows through a turbulator strip it constantly encounters flow contractions and expansions as a result of the alternating rows which are out of phase with each other, refer to Figure 3. The loss coefficients for a sudden contraction and a sudden expansion which the fluid experiences as it passes between the turbulator blades may be computed from the classic expressions reported in most fluid texts, *e.g.*,

White (1987). The following expressions:

$$K_{SC} \approx 0.42(1-\sigma^2) \tag{48}$$

and

$$K_{SE} = (1-\sigma^2)^2 \tag{49}$$

are used to model the pressure drop which is a result of the sudden contraction and expansion within the turbulator geometry, where $K = \Delta p/(1/2\rho\overline{w}^2)$ and $\sigma = A_i/A_o < 1$ is the area or blockage ratio. In most typical turbulator applications, the turbulator is composed of alternating rows which have the same width, *i.e.*, $\beta = 0.5$. Thus, the total contribution of the expansion and contraction losses is found to be

$$K_{\text{eff}} \approx 0.878 \tag{50}$$

This value is also in agreement with values computed from graphical results reported in Kays and London (1984) for loss coefficients of tube bundles and parallel plate channels for various flow conditions.

Substituting the expressions for the form drag, Eq. (46), and effective loss coefficient, Eq. (50), derived earlier into Eq. (11), along with the turbulent skin friction component on the channel wall leads to

$$f_{\text{tur}} = 0.074\left(Re_{d_h}\frac{\lambda}{d_h}\right)^{-1/5}\left(\frac{1}{F_w}\right) + \left(1.2\frac{(\pi+4)\sin^2(\theta)}{\pi+4\sin(\theta)} + 0.878\sin(\theta)\right)F_f \tag{51}$$

The ratio of $A_{\text{front}}/A_{\text{fins}} = \sin(\theta)/2$ and $A_{\text{drag}}/A_{\text{fins}} = 1/2$, where the surface area of a single fin is taken to be $A_{\text{fin}} = 2HW/\sin(\theta)$ and $A_{\text{drag}} = HW/\sin(\theta)$, recalling that the potential flow solution for the drag coefficient for an inclined lamina, Eq. (45), is based upon the chord length rather than the profile height. This expression was found to be in good agreement with the trends observed in the experimental data for both small angles of inclination and nearly vertical obstructions.

At higher Reynolds numbers it is assumed that the region between fins is fully occupied by a pair of symmetric recirculation bubbles. The average value of the heat transfer coefficient for both the fin surface and the channel walls is taken to be

$$j_{\text{tur}} = 0.191\left(Re_{d_h}\frac{W}{d_h}\right)^{-1/3} \tag{52}$$

Equation (52) has the same order of magnitude and Reynolds number exponent as the expression obtained from the numerical results of Patankar *et al.* (1977), Eq. (2).

Transition Region Model

The creeping flow, laminar boundary layer, and turbulent region models are plotted in Figure 5 along with experimental data for a typical turbulator geometry. These asymptotic relations may now be combined in the form of Eqs. (6) and (7) to develop models which are valid over the entire range of Reynolds numbers. The correlation parameters have been found to be $m \approx 1$ and $n \approx 6/7$ in Eq. (6), while in Eq. (7), $p \approx 9/2$ and $q \approx 7/5$ for turbulators with a straight profile, *i.e.*, square or trapezoidal, and $q \approx 5$ for turbulators with a curved profile, *i.e.*, sinusoidal or rounded.

Turbulator strips which have a curved profile allow the flow to become more three dimensional as compared to those having a straight profile which tend to make the flow more two dimensional. As a result, the heat transfer coefficients are higher for the straight profiles, thus the correlation parameter for the laminar and turbulent regions must be smaller for the straight profiles and larger for the curved profiles when interpolating in the transition region.

Examination of the models reveals that the important parameters affecting the flow are the wave length of the convolutions λ, the surface area enhancement factor F_w, fin area factor F_f, fin width W, fin angle $\theta = \tan^{-1}(2H/\lambda)$ as a function of the

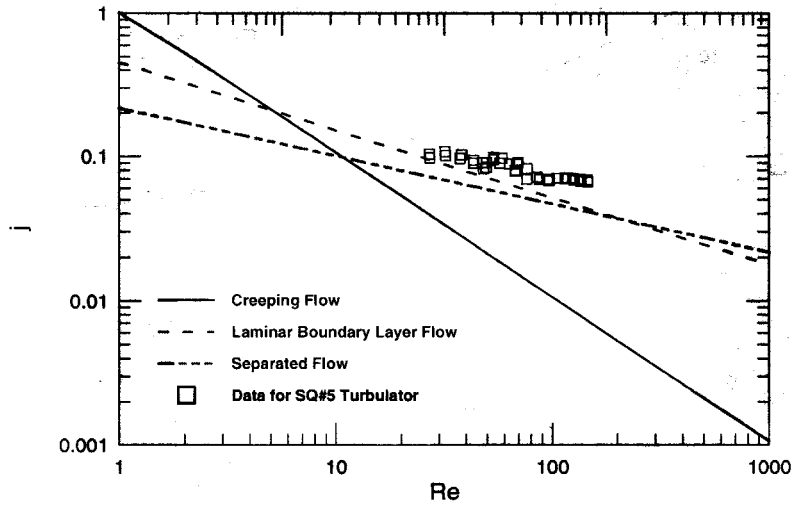

FIGURE 5 Asymptotic limits of Colburn j factor.

channel spacing H, and the hydraulic diameter of the enhanced channel d_h. The fin thickness t is generally much smaller than the other characteristic dimensions and is not explicitly modelled as it contributes less than 5 percent of the total surface area. The effects of fin edge surface area are however, included through the scale factors F_w and F_f. The hydraulic diameter of the channel is defined as $d_h = 4V_{\text{free}}/A_{\text{wet}}$. In terms of the geometrical parameters

$$d_h = \frac{4(\lambda HW)\phi}{8S_oW + 2\lambda W + 8S_ot} \tag{53}$$

where,

$$\phi = 1 - \frac{4S_ot}{\lambda H} \tag{54}$$

is the porosity.

COMPARISON OF MODELS WITH DATA

Experimental Program

Experimental data for ten turbulator configurations were obtained by Muzychka (1999). The experimental apparatus consisted of an a shell and tube type heat exchanger. The aluminum test section contained four 11 inch by 1 inch turbulator strips. The important characteristics of these devices are reported in Table I. Details of the particular dimensions of the turbulator strips examined cannot be given due to proprietary issues. However, the nominal range for the particular dimensions are: $4\,\text{mm} < \lambda < 12\,\text{mm}$, $20° < \theta < 90°$, $1\,\text{mm} < W < 2\,\text{mm}$, and $2\,\text{mm} < H < 3.5\,\text{mm}$. The test fixture was operated in a counterflow arrangement using automatic transmission oil as a test fluid and a 50 percent water 50 percent glycol solution as the coolant. Experiments were conducted at two temperature levels in order that Prandtl number effects be examined as well as to provide for a wider Reynolds number range. The resulting Prandtl numbers were $Pr = 85$ and $Pr = 150$. Details of the experiments are found in Muzychka (1999).

Data were obtained for the ten turbulators summarized in Table I. Results for the f and j factors are presented in Figures 6a–6j. Experimental uncertainties were determined using the root sum square method (Moffat, 1988). The uncertainties in the Fanning friction factor and Reynolds number were determined to be 3.2 percent and 1.2 percent, respectively. The uncertainties in the Colburn j factor and Nusselt

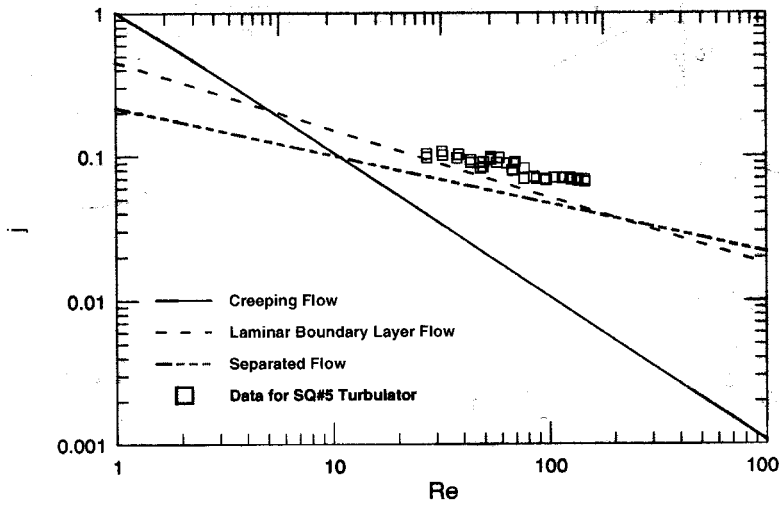

FIGURE 5 Asymptotic limits of Colburn j factor.

channel spacing H, and the hydraulic diameter of the enhanced channel d_h. The fin thickness t is generally much smaller than the other characteristic dimensions and is not explicitly modelled as it contributes less than 5 percent of the total surface area. The effects of fin edge surface area are however, included through the scale factors F_w and F_f. The hydraulic diameter of the channel is defined as $d_h = 4V_{\text{free}}/A_{\text{wet}}$. In terms of the geometrical parameters

$$d_h = \frac{4(\lambda HW)\phi}{8S_oW + 2\lambda W + 8S_ot} \tag{53}$$

where,

$$\phi = 1 - \frac{4S_ot}{\lambda H} \tag{54}$$

is the porosity.

COMPARISON OF MODELS WITH DATA

Experimental Program

Experimental data for ten turbulator configurations were obtained by Muzychka (1999). The experimental apparatus consisted of an a shell and tube type heat exchanger. The aluminum test section contained four 11 inch by 1 inch turbulator strips. The important characteristics of these devices are reported in Table I. Details of the particular dimensions of the turbulator strips examined cannot be given due to proprietary issues. However, the nominal range for the particular dimensions are: $4\,\text{mm} < \lambda < 12\,\text{mm}$, $20° < \theta < 90°$, $1\,\text{mm} < W < 2\,\text{mm}$, and $2\,\text{mm} < H < 3.5\,\text{mm}$. The test fixture was operated in a counterflow arrangement using automatic transmission oil as a test fluid and a 50 percent water 50 percent glycol solution as the coolant. Experiments were conducted at two temperature levels in order that Prandtl number effects be examined as well as to provide for a wider Reynolds number range. The resulting Prandtl numbers were $Pr = 85$ and $Pr = 150$. Details of the experiments are found in Muzychka (1999).

Data were obtained for the ten turbulators summarized in Table I. Results for the f and j factors are presented in Figures 6a–6j. Experimental uncertainties were determined using the root sum square method (Moffat, 1988). The uncertainties in the Fanning friction factor and Reynolds number were determined to be 3.2 percent and 1.2 percent, respectively. The uncertainties in the Colburn j factor and Nusselt

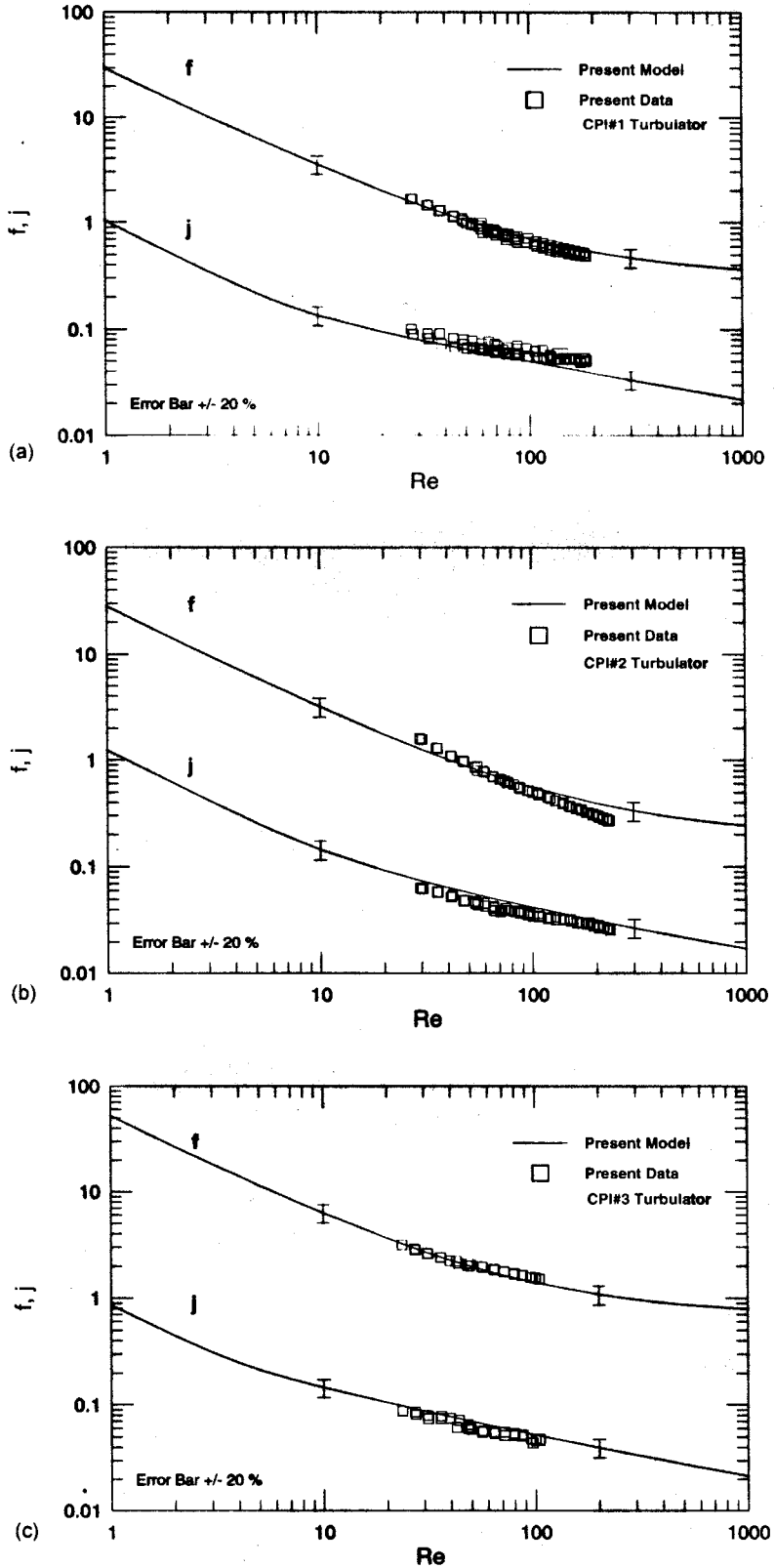

FIGURE 6 Comparisons of turbulator strip data with model.

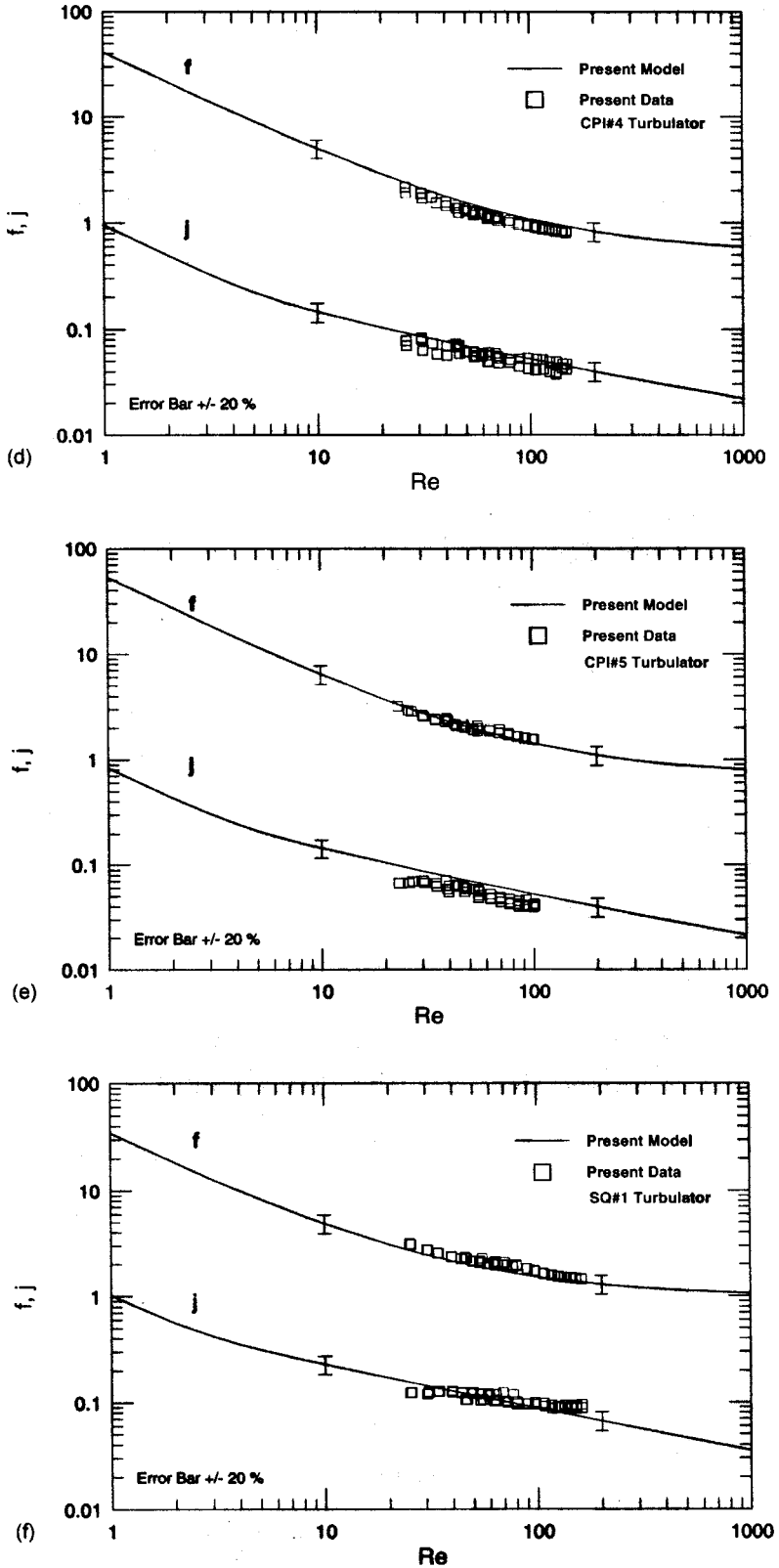

FIGURE 6 (Continued).

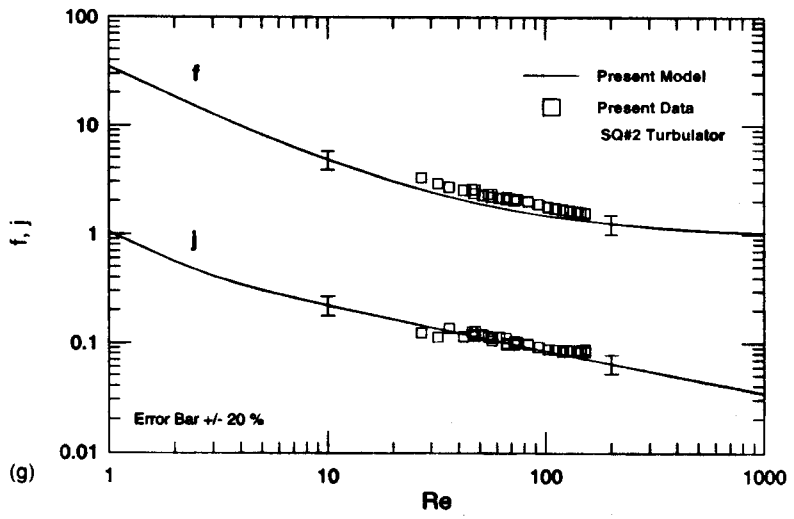

(g)

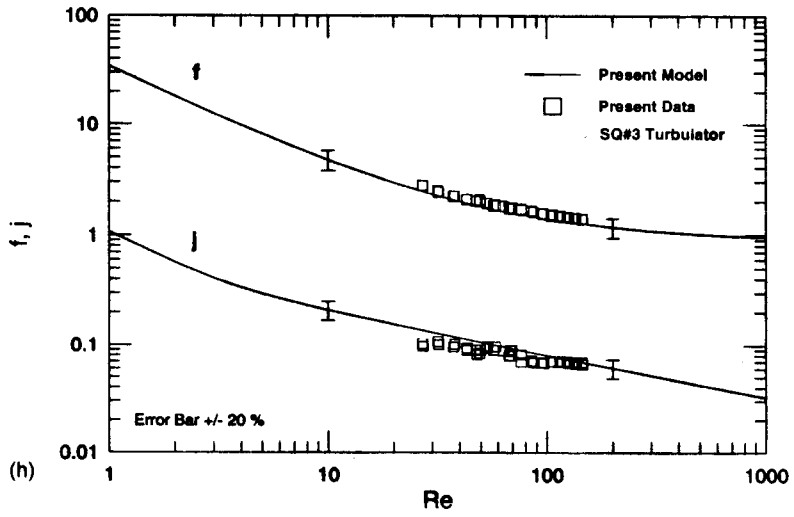

(h)

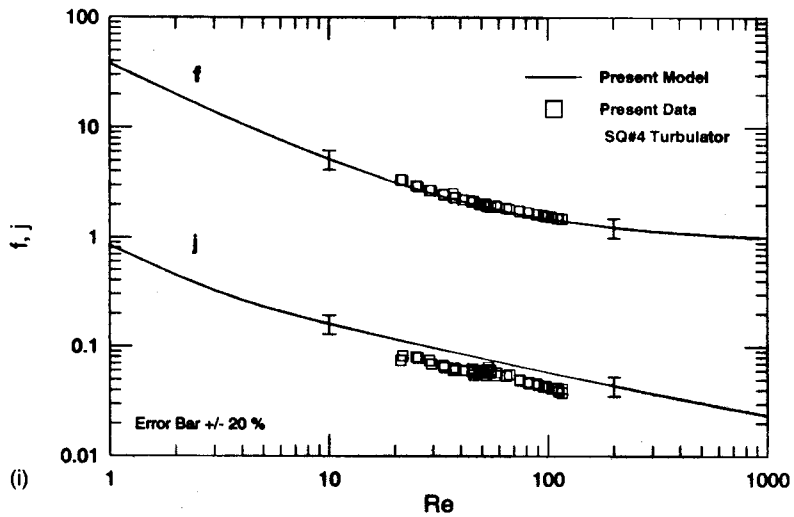

(i)

FIGURE 6 (Continued).

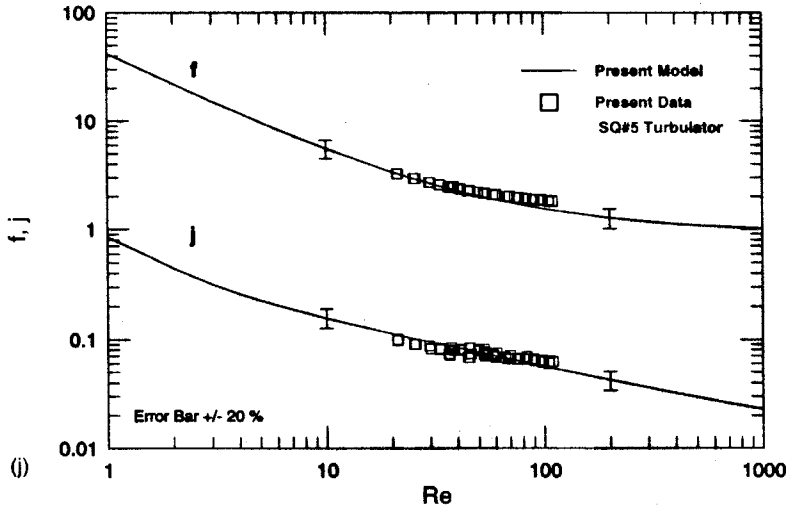

FIGURE 6 (Continued).

numbers were determined to be 7.3 – 13.0 percent and 7.2 – 12.9 percent, respectively. The upper limit in the j and Nu parameters is a result of smaller temperature differences being recorded for the lower oil inlet temperature tests.

RESULTS

The proposed models are compared with ten sets of data for the turbulator configurations which are reported in Table I. Table II presents a summary of the optimal value of the correlation parameters for combining the creeping flow, laminar boundary layer and turbulent boundary layer models for each set of data. The values reported in Table II minimize the root mean square (RMS) differences between the model predictions and the experimental data. Excellent correlation is obtained for the friction factor data for all configurations tested. Good agreement between the proposed model and the turbulator data is also achieved for the Colburn j factor. The correlation parameters for the $CPI-2$ device were not tabulated, since this device is a special case of the $CPI-1$ device. The $CPI-2$ device has the same geometric configuration as the $CPI-1$ device except that every fourth row is replaced by a neutral surface containing no convolutions.

TABLE II Comparison of models with data using optimal values of blending parameters

	f			j		
Device	m	n	RMS	p	q	RMS
CPI – 1	1	0.99	5.80	3.0	4.0	10.21
CPI – 2	–	–	–			
CPI – 3	1	0.85	4.23	4.0	5.0	13.42
CPI – 4	1	1.00	3.95	5.0	5.0	17.69
CPI – 5	1	0.87	4.85	5.0	5.0	29.50
SQ – 1	1	0.79	3.59	5.0	1.25	12.31
SQ – 2	1	0.71	2.98	5.0	1.25	7.82
SQ – 3	1	0.80	1.49	5.0	1.75	9.97
SQ – 4	1	0.85	2.11	4.5	5.0	35.92
SQ – 5	1	0.81	5.27	5.0	4.0	9.37

Table III presents the RMS and (min/max) values of the percent differences for the case where fixed values of the correlation parameters are used for all cases. The majority of the friction factor and Colburn j factor data are predicted within ± 20 percent. The large RMS difference reported for the $CPI-5$ and $SQ-4$ devices represents an average value of a biased error. All of the data for these two devices fall short of the model predictions, however, the model predicts the correct trends.

TABLE III Comparison of models with data with fixed values of blending parameter

	f ($m=1$, $n=6/7$)		j ($p=9/2$,$q^\dagger$)	
Device	RMS	(min/max)	RMS	(min/max)
CPI – 1	8.25	−16.70/7.12	16.27	0.38/26.66
CPI – 2	18.12	−37.50/20.08	17.44	−29.28/−7.70
CPI – 3	6.57	−2.70/10.30	13.37	−22.31/−3.38
CPI – 4	16.89	−29.98/−10.16	17.72	−34.98/4.28
CPI – 5	5.94	−6.36/12.27	29.53	−41.18/−10.27
SQ – 1	11.50	6.40/18.05	12.06	−25.47/23.20
SQ – 2	18.88	14.58/23.97	8.95	−19.90/18.26
SQ – 3	9.44	7.00/12.46	17.99	−28.95/−0.40
SQ – 4	5.84	2.59/11.25	35.90	−52.41/−17.40
SQ – 5	10.76	−0.30/17.91	9.38	−21.13/12.97

† $q=7/5$ for straight profiles, $q=5$ for curved or rounded profiles.

Figures 6a–6j compare the proposed models with the turbulator data of Muzychka (1999). It is clear from Figures 6a–6j that the proposed model captures the correct physical behavior of the experimental data. With the exception of two j data sets, in which the data fall short of the model, excellent agreement between the proposed model and experimental data is achieved over the range of data. Further, validation of the proposed models is required at higher Reynolds numbers.

SUMMARY AND CONCLUSIONS

Models were developed for predicting the friction and heat transfer characteristics of the turbulator strip. This device is utilized in many automotive heat exchangers. Unfortunately, due the proprietary nature of these devices, performance characteristics are not published and hence models are not readily available. These new models fulfill the need for predictive techniques for these thermal enhancement devices. The proposed models were developed by combining asymptotic expressions for three characteristic flow regimes; creeping flow, laminar boundary layer, and turbulent boundary layer or completely inertial flow. Model predictions agree within ± 20 percent for 92 percent of friction factor data and 71 percent for Colburn j factor data for the experimental data obtained for this work.

Acknowledgements

The authors acknowledge the financial support of DANA Corporation – Long Manufacturing Division of Oakville, Ontario and the Natural Sciences and Engineering Research Council of Canada.

NOMENCLATURE

A	area, m^2
c_p	heat capacity, J/kgK
C_o	Kozeny coefficient
C_D	drag coefficient
C_f	skin friction coefficient, $\equiv \overline{\tau}/((1/2)\rho\overline{w}^2)$
d_h	hydraulic diameter, $\equiv 4V_{\text{free}}/A_{\text{wet}}$
$\mathrm{E}(\cdot)$	complete elliptic integral second kind
f	friction factor, $\equiv \overline{\tau}/((1/2)\rho\overline{w}^2)$
H	channel or fin height, m
h	heat transfer coefficient, W/m^2K
j	Colburn factor, $\equiv StPr^{2/3}$
K_e, K_c	expansion/contraction loss coefficient
K_{eff}	effective loss coefficient
k	thermal conductivity, W/mK
k_o	Kozeny constant, ≈ 2.5
L	length of channel, m
L_e	tortuous or effective flow length, m
L_f	interrupted fin length, m
m	Falkner-Skan wedge parameter
$\dot{m}$	mass flow rate, kg/s
m, n, p, q	correlation parameters
Nu_{d_h}	Nusselt number, $\equiv hd_h/k$
p	pressure, Pa
Pr	Prandtl number, $\equiv \nu/\alpha$
Q	heat transfer, W
Re_{d_h}	Reynolds number, $\equiv \overline{w}d_h/\nu$
S_o	effective fin length, m
t	fin thickness, m
T	temperature, K
U	overall heat transfer coefficient, W/m^2K
V	volume, m^3

$\overline{w}$	average velocity, m/s
W	fin width, m
X	chord length, m

Greek Symbols

α	thermal diffusivity, m^2/s
β	Falkner-Skan wedge parameter
η	efficiency
λ	wavelength, m
μ	dynamic viscosity, Ns/m^2
ν	kinematic viscosity, m^2/s
ϕ	porosity, V_{free}/V_{total}
ρ	fluid density, kg/m^3
σ	frontal area ratio, $\equiv (A_{free}/A_{front})$
τ	wall shear stress, N/m^2
θ	fin angle, rad

Subscripts

cf	creeping flow
d_h	based upon hydraulic diameter
eff	effective
f	fin
FP	flat plate
lam	laminar
PS	plane stagnation
tur	turbulent
w	wall
x	local value

References

Bejan, A. (1995) *Convection Heat Transfer*, Wiley, New York.

Bergles, A. E. (1985) Chapter 3: Techniques to Augment Heat Transfer, In: *Handbook of Heat Transfer Applications*, Eds. Rohsenow, W. M., Hartnett, J. P. and Ganic, E. N., McGraw-Hill, New York.

Bird, R. B., Stewart, W. E. and Lightfoot, E. N. (1960) *Transport Phenomena*, Wiley, New York.

Blevins, R. D. (1984) *Applied Fluid Dynamics Handbook*, Van Nostrand Reinhold, New York.

Burmeister, L. C. (1993) *Convective Heat Transfer*, Wiley, New York.

Carman, P. C. (1956) *Flow of Gases Through Porous Media*, Butterworths Scientific Publications, London.

Cebeci, T. and Bradshaw, P. (1984) *Physical and Computational Aspects of Convective Heat Transfer*, Springer-Verlag, New York.

Churchill, S. W. (1988) *Viscous Flows: The Practical Use of Theory*, Butterworths, Boston, MA.

Churchill, S. W. and Usagi, R. (1972) "A General Expression for the Correlation of Rates of Transfer and Other Phenomena", *American Institute of Chemical Engineers*, **18**, 1121–1128.

Happel, J. and Brenner, H. (1965) *Low Reynolds Number Hydrodynamics*, Noordhoff International Publishing.

Happel, J. and Brenner, H. (1965) *Low Reynolds Number Hydrodynamics*, Noordhoff International Publishing.

Igarashi, T. (1985) "Heat Transfer from a Square Prism to an Air Stream", *International Journal of Heat and Mass Transfer*, **28**, 175–181.

Igarashi, T., Hirata, M. and Nishiwaki, N. (1975) "Heat Transfer in Separated Flows: Part 1, Experiments on Local Heat Transfer from the Rear of a Flat Plate Inclined to an Air Stream", *Heat Transfer, Japanese Research*, **4**, 11–32.

Joshi, H. M. and Webb, R. L. (1987) "Heat Transfer and Friction in the Offset Strip Fin Heat Exchanger", *International Journal of Heat and Mass Transfer*, **30**, 69–84.

Kalinin, E. K. and Dreitser, G. A. (1998) "Heat transfer Enhancement in Heat Exchangers", In: *Advances in Heat Transfer*, Eds. Hartnett, J. P., Irvine, T. F., Cho, Y. I. and Greene, G. A., pp. 159–332, Academic Press, New York.

Kays, W. M. and Crawford, M. E. (1993) *Convective Heat and Mass Transfer*, McGraw-Hill, New York.

Kays, W. M. and London, A. L. (1984) *Compact Heat Exchangers*, McGraw-Hill, New York.

Knudsen, J. G. and Katz, D. L. (1958) *Fluid Dynamics and Heat Transfer*, McGraw-Hill, New York.

Lamb, H. (1932) *Hydrodynamics*, Cambridge University Press.

Milne-Thomson, L. M. (1968) *Theoretical Hydrodynamics*, Dover.

Moffat, R. J. (1988) "Describing Uncertainties in Experimental Results", *Experimental Thermal and Fluid Science*, **1**, 3–17.

Muzychka, Y. S. (1999) *Analytical and Experimental Study of Fluid Friction and Heat Transfer in Low Reynolds Number Flow Heat Exchangers, Ph.D. Thesis*, University of Waterloo, Waterloo, ON.

Nield, D. A. and Bejan, A. (1992) *Convection in Porous Media*, Springer-Verlag, New York.

Patankar, S. V., Liu, C. H. and Sparrow, E. M. (1977) "Fully Developed Flow and Heat Transfer in Ducts Having Streamwise Periodic Variations of Cross-sectional Area", *Journal of Heat Transfer*, **99**, 180–186.

Schlichting, H. V. (1979) *Boundary Layer Theory*, McGraw-Hill, New York.

Shah, R. K. and London, A. L. (1978) *Laminar Flow Forced Convection in Ducts*, Academic Press, New York.

Sridhar, S. (1995) *Heat Transfer and Pressure Drop in Flows Perpendicular to an Offset Fin Structure, Ph.D. Thesis*, University of Maryland.

Webb, R. L. (1987) Chapter 17: Enhancement of Single Phase Heat Transfer, In: *Handbook of Single Phase Convective Heat Transfer*, Eds. Kakac, S., Shah, R. K. and Aung, W., Wiley, New York.

Webb, R. L. (1994) *Principles of Enhanced Heat Transfer*, John Wiley, New York.

White, F. M. (1987) *Fluid Mechanics*, McGraw-Hill, New York.

White, F. M. (1991) *Viscous Fluid Flow*, McGraw-Hill, New York.